

DESY Summer Student Programme 2015 Report: 3-beam X-ray Diffraction Simulation Testing

Roxanna Barry,
University of Glasgow,
United Kingdom



September 9, 2015

Abstract

Since synchrotron radiation from storage rings has been utilised in the production of high intensity, bright X-ray beams, the study of the structure of matter using X-ray diffraction has improved dramatically. This report outlines the theory behind X-ray diffraction and discusses the testing of a 3-beam X-ray diffraction simulation produced in 1994, comparing it's results with a more recent programme in *Mathematica*.

Contents

1. Introduction	1
2. X-Ray Diffraction: Dynamical Theory	3
2.1. X-Ray Diffraction	3
2.2. Elementary Dynamical Theory	4
2.3. Additional Equations	6
3. Simulation Testing	7
3.1. "Multi" Program	7
3.2. Results	7
3.2.1. Future Work	9
3.3. Creating a new Input file	10
References	11
Appendices	12
A. Mathematica Function	12

1. Introduction

X-rays were first discovered by Wilhelm C. Röntgen in 1895 while examining the discharge from electrodes in an evacuated glass tube. He observed faint light from a fluorescent screen placed near the tube and found that, when placing his hand between the tube and the screen, he could see the bones inside. He photographed this phenomena using his wife's hand, providing scientific documentation of his discovery, as shown in Figure 1. X-ray imaging like this is based on X-ray absorption being dependent on the atomic number of the elements the ray is interacting with. Another important application of X-rays is diffraction phenomena, which was not realised until 1912 when von Laue et al. obtained the first diffraction pattern from a crystal of copper sulfate. This was a key event triggering a dramatic development in scientific research into the structure of matter, utilising X-rays to analyse the atomic structure of crystalline materials. Von Laue et al. were able to show how crystalline matter is built up by atoms forming a periodic lattice. Since the discovery of X-rays, they have been shown to be an invaluable tool for investigating the structure of matter, including the celebrated discovery of the double helix structure of DNA in 1953 due to the combined efforts of Franklin, Watson and Crick. In turn this use of X-rays has been important not only in scientific research but also in contemporary technology.



Figure 1: X-ray image captured by Röntgen of his wife's hand [1].

Synchrotron radiation describes the radiation from charged particles forced to travel along curved paths by applied magnetic fields, travelling at relativistic speeds. This can be produced in storage rings (Figure 2), either in the bending magnets which keep electrons in a circular orbit, or in insertion devices such as undulators placed at the straight sections of the ring. In devices such as undulators, an alternating magnetic field induces the electron into an oscillatory path rather than a straight line.

Initially, synchrotron radiation occurred as a nuisance, causing undesirable energy loss during particle physics research. However, the usefulness of this radiation production was soon realised and in modern X-ray research, most sources of synchrotron radiation are storage rings. Previously, the source of X-ray production was the main limitation

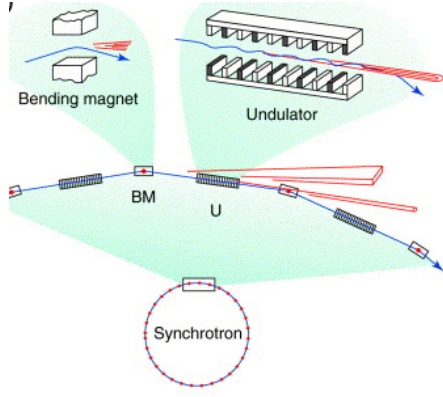


Figure 2: Example set up of a storage ring producing synchrotron radiation [2].

of exploring the structure of matter, until the 1970s when the synchrotron radiation produced from charged particles circulating in storage rings was realised to be a more intense and versatile source of X-rays. This has resulted in synchrotron sources which are approximately a factor of 10^{12} times brighter than earlier lab-based sources and hence the pace of innovation in X-ray science increased significantly to what is used today.

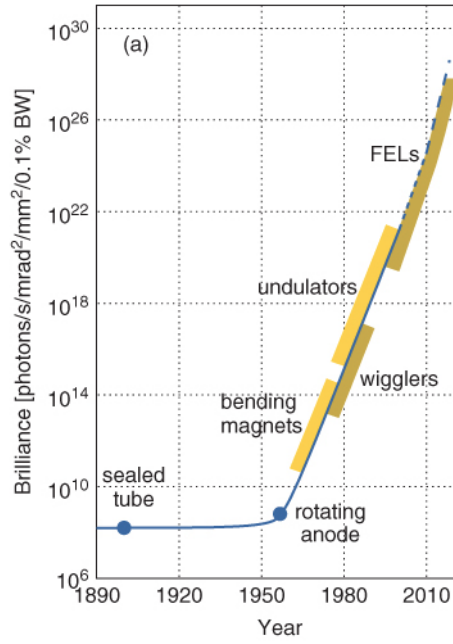


Figure 3: History of X-ray brilliance [2].

2. X-Ray Diffraction: Dynamical Theory

2.1. X-Ray Diffraction

Crystalline materials are such that the atoms are arranged in a regular pattern, and there exists a minimal volume element which describes the crystal through periodic repetition in three dimensions. This volume element is called the unit cell, described by the axes **a**, **b** and **c**, with angles between them α , β and γ . The planes of atoms are spaced a distance d apart. When X-rays interact with a crystalline substance, a diffraction pattern is obtained. For a pure substance, the diffraction pattern is similar to a fingerprint of the substance, being unique specifically to the material being examined.

William Lawrence Bragg and William Henry Bragg first proposed the Bragg formulation of X-ray diffraction in 1913 after their discovery that crystalline solids produced interesting patterns of reflected X-rays. Their research found that at specific wavelengths and incident angles, the crystals produced intense peaks of reflected radiation. Bragg diffraction supplies the angles for both coherent and incoherent scattering from a crystal lattice, by analysing the wave interference (diffraction) pattern produced by re-emitted wave fields interfering with each other, either constructively or destructively.

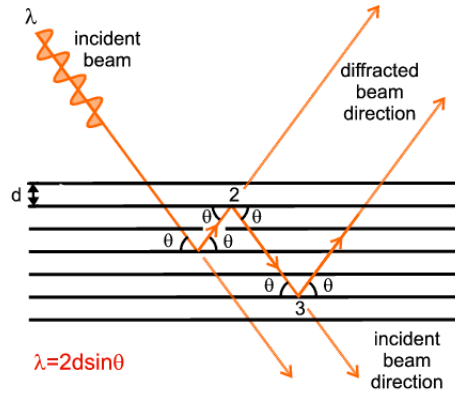


Figure 4: Bragg's Law on Diffraction [3].

This Bragg diffraction occurs when the wavelength is comparable to the atomic spacings of the crystal and the radiation is scattered in a specular fashion by the atoms, undergoing constructive interference. Constructive interference demands the waves remain in phase, with the path length being an integer multiple of the wavelength, which is outlined in Figure 4. The effect of the interference intensifies due to the cumulative effect of reflection in additional planes of the crystalline lattice leading to Bragg's law, defined in Equation 1, outlining the condition on θ for constructive interference.

$$n\lambda = 2d\sin(\theta) \quad (1)$$

Here, λ is the wavelength of the incident wave, d is the lattice spacings as shown in Figure 4 and n is a positive integer. In diffraction patterns, strong intensities called

Bragg peaks can be observed at points where the scattering angles satisfy the Bragg condition.

To describe the crystallographic planes in either laboratory space or reciprocal space, one uses the Miller notation. Miller indices are a notation system for planes in crystal lattices, with a family of lattice planes being defined by the three Miller indices, h , k and l , written (hkl) . These define the family of planes *orthogonal* to

$$h\mathbf{a} + k\mathbf{b} + l\mathbf{c}$$

where \mathbf{a} , \mathbf{b} and \mathbf{c} are the basis vectors of the reciprocal lattice. The constants h , k and l are the reciprocals of the fractional intercepts of the \mathbf{a} , \mathbf{b} and \mathbf{c} axes of the unit cell - i.e. the intercepts which the plane makes with the crystallographic axes. Some examples are pictured in Figure 5.

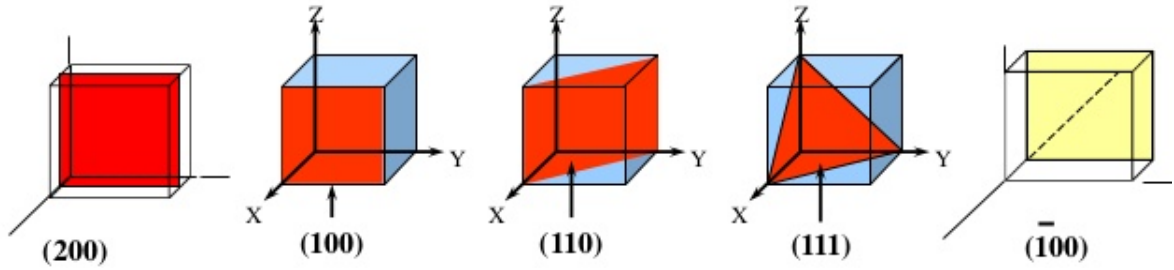


Figure 5: Examples of Miller indices and their planes [4].

Laue developed a simple theory of three-dimensional X-ray diffraction, called Kinematical (or geometrical) theory. However, the Kinematical theory of X-ray diffraction only considers the materials atoms interacting with the primary (refracted) wave in the crystal. Therefore, it neglects interactions with the part of the wave field arising from the collective scattering due to the other atoms, i.e. the theory ignores the interaction between the refracted wave and the diffracted ones. This theory is a good approximation when considering highly imperfect crystals, constructed with small mosaic blocks, however for imperfect crystals the theory breaks down when comparing theoretical results to experimental results, thus a more rigorous theory, called Dynamical theory, is required.

2.2. Elementary Dynamical Theory

Darwin (1914b) was first to point out the inaccuracy of the Kinematical theory and its violation of the conservation of energy [6]. This is because the Kinematical theory assumes the amplitude of the wave arriving at each diffracting centre in the crystal is the same, neglecting the interaction of the wave with matter, not taking into account the energy which has already been reflected by previous layers in the crystal. This theory doesn't account for the interaction of diffracted waves with the refracted wave, disregarding multiple scattering effects. Additionally, the Kinematical theory doesn't provide any phase information about the processes inside the crystal. To understand the

diffraction of perfect, or close to perfect, crystals, the dynamical theory is necessary, since to explain the formation of defect images in diffraction patterns requires information on the propagation of the beam inside the crystal, not just the global intensity diffracted by the X-rays. However, the results from the Dynamical theory tend asymptotically towards those of the Kinematical theory when the crystal thickness is much smaller than a certain length called Pendellösung distance.

The first Dynamical theory of X-ray diffraction was developed by C. G. Darwin in 1914, in which the crystal is considered to be an infinite stack of atomic planes, each causing a weak reflected wave, with a possibility of the direction of re-scattering being the same as that of the incident beam. Additionally, both Ewald and Laue have outlined a Dynamical theory of X-ray diffraction. Ewald's approach discusses the interaction of a electromagnetic wave with a distribution of discrete dipoles, while Laue's assumption (1931, 1960) considers the electric negative and positive charges being distributed in a continuous way throughout the volume of the crystal. The distribution is such that the total charge cancels out and the crystal is neutral, and the local electric charge and density of current are also zero.

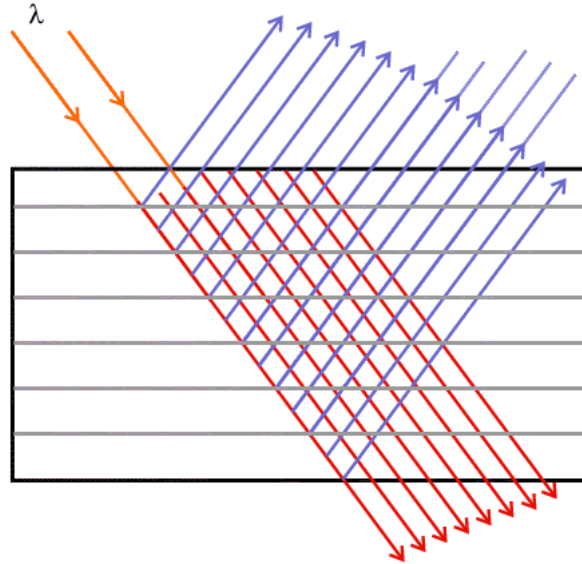


Figure 6: Illustration of multiple diffraction in a perfect crystal [3].

Away from the simplistic assumption that each individual diffraction event acts independently of others, the Dynamical theory accounts for multiple scattering effects. When the incident wave propagates down into the (perfect) crystal, a small fraction is reflected as it passes each atomic plane, which in turn decreases the amplitude of the wave. There is also a chance of the reflection being re-scattered in the direction of the incident beam prior to leaving the crystal. If the X-ray beam is incident at the Bragg angle θ , it will be reflected at the angle θ and the diffracted ray will continue to satisfy Bragg's law, enabling it to diffract a second time in the direction of the original incident beam (and

perhaps a third time, and so on). This is shown in Figure 4 in the previous section. If the whole crystal is bathed in X-rays, all of the waves, subject to multiple diffraction, can interfere with each other. Ewalds described this process in his Dynamical theory, in which the diffraction intensity, I , is proportional to the magnitude of the structure factor, F . This Dynamical diffraction is illustrated in Figure 6.

2.3. Additional Equations

When X-rays, short-wavelength electromagnetic waves, interact with matter, they excite electrons which oscillate and behave like dipoles. The wave equation in both Ewald's and Laue's Dynamical theories of X-ray diffraction is derived based on the properties of electromagnetic waves' interaction with matter. The electromagnetic field is represented by the electric field, \mathbf{E} , and the magnetic induction, \mathbf{B} . These are also related locally to the electric displacements, \mathbf{D} , and the magnetic field, \mathbf{H} , by material relations (describing the reaction of a linear medium to the electromagnetic field):

$$\begin{aligned}\mathbf{D} &= \epsilon \mathbf{E} = \epsilon_0 \mathbf{E} + \mathbf{P} \\ \mathbf{B} &= \mu \mathbf{H} = \mu_0 (\mathbf{H} + \mathbf{M})\end{aligned}$$

where ϵ and μ are the dielectric constant and magnetic permeability of the medium, respectively, with ϵ_0 and μ_0 referring to the same constants in a vacuum. \mathbf{P} is the electric polarisation and \mathbf{M} the magnetisation [6].

In a continuous medium, the space and time derivatives of \mathbf{E} , \mathbf{B} , \mathbf{D} , \mathbf{H} , \mathbf{j} (electric current density, $\mathbf{j} = \sigma \mathbf{E}$, σ specific conductivity) and of the local electric charge density ρ are related by *Maxwell's equations*

$$\begin{aligned}\text{curl} \mathbf{H} &= \frac{\delta \mathbf{D}}{\delta t} + \mathbf{j}, \\ \text{curl} \mathbf{E} &= -\frac{\delta \mathbf{B}}{\delta t}, \\ \text{div} \mathbf{D} &= \rho, \\ \text{div} \mathbf{B} &= 0.\end{aligned}$$

The *fundamental equations* of Dynamical theory, as named by Laue, is the set of equations

$$\Psi_h = \frac{k^2}{K_h^2 - k^2} \sum_{\mathbf{h}'} \chi_{h-h'} \Psi_{h'} \quad (2)$$

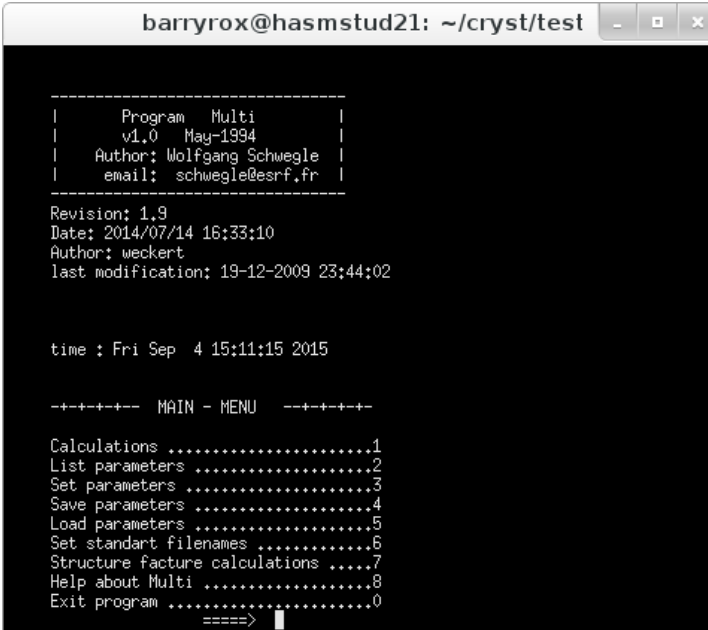
where k is the wave number in vacuum, K_h is the wave vector of the wave field, χ is the Fourier component of dielectric susceptibility and Ψ is the rotation angle around the reciprocal lattice vector.

3. Simulation Testing

3.1. "Multi" Program

To simulate n -beam diffraction, and measure its reflectivities, a program *Multi* was written in 1994 by Wolfgang Schwegle, with the most recent modification being in 2009. The source code is written in *FORTRAN* and was compiled using *ifort2015*. The program is developed using the Dynamical theory of X-ray diffraction and has the potential to calculate structure factors along with the reflectivities of a crystal for varying ω or Ψ angles and even varying values of energy.

The program receives information from two input files containing information on all the parameters required for its calculations. The parameters include actual values of the psi angle, omega angle, specific wavelength and miller indices of the considered n reflections along with the surface normal *into* the crystal, crystal thickness and polarisation angle. For the calculation of reflectivities for the scans available (ω , Ψ and energy), *Multi* creates an output file, *multi.refl*, which stores the data. The scan parameter is in the first column, and the reflectivities of each reflection in the following columns. This allows easy plotting of the data against the chosen scan variable.



```
barryrox@hasmstud21: ~/cryst/test

-----
|      Program  Multi      |
|      v1.0   May-1994    |
|  Author: Wolfgang Schwegle |
|  email:  schwegle@esrf.fr |
|-----|
Revision: 1.9
Date: 2014/07/14 16:33:10
Author: weckert
last modification: 19-12-2009 23:44:02

time : Fri Sep  4 15:11:15 2015

--++-- MAIN - MENU --++--

Calculations .....1
List parameters .....2
Set parameters .....3
Save parameters .....4
Load parameters .....5
Set standart filenames .....6
Structure facture calculations .....7
Help about Multi .....8
Exit program .....0
====>
```

Figure 7: Home screen of Multi program

3.2. Results

The program *Multi* was tested by comparing results of reflectivities with another program *Crystallography*, written by Martin Tolkiehn, based on the Dynamical theory's

mathematical calculations of structure factors in *Authier*. Currently, the program is unable to calculate structure factors internally, so the tests were run using pre-set structure factors calculated using the program *Crystallography*. Results for Germanium, Silicon and Gallium Arsenate are discussed below.

The program was tested for 2-beam diffraction, as the 2-beam case was easily comparable with the results from the Dynamical theory outlined in *Authier*. However, it was found that the program was unable to simulate 2-beam diffraction. Hence 3-beam diffraction was used and the tests were run with Pi polarisation and $\Psi = -1000\text{arcsec}$. This value of Ψ allowed the reflectivities to be calculated as if it were a 2-beam case, permitting the comparison between the results obtained from *Multi* and those from the Dynamical theory.

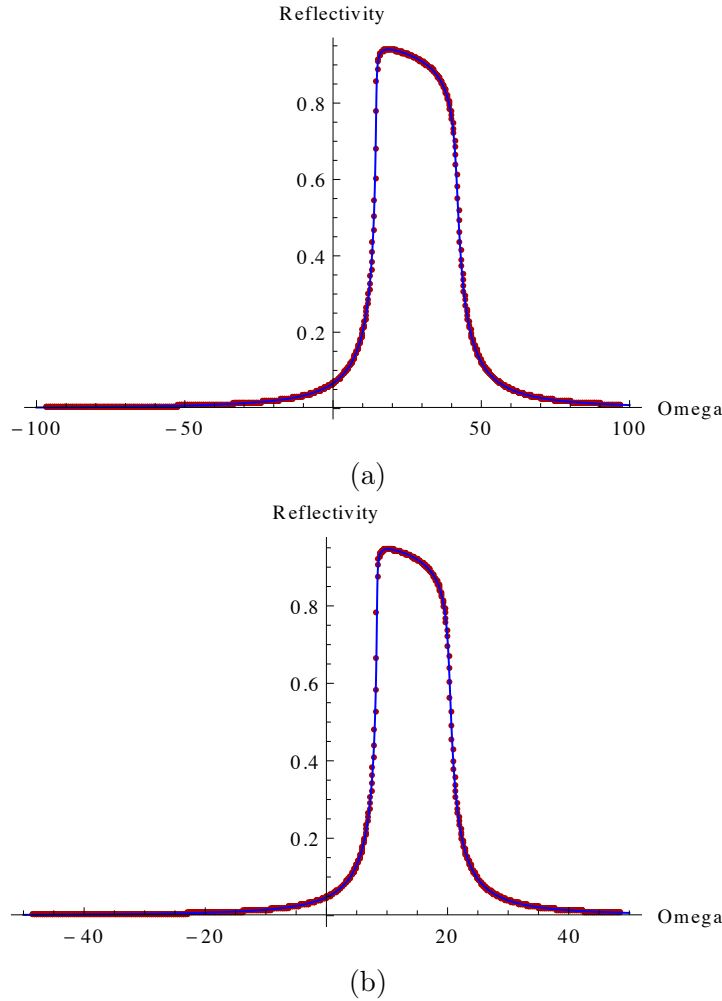


Figure 8: (a) Germanium (*Ge*), and (b) Silicon (*Si*).

Figure 8 displays data for the elements of Germanium and Silicon obtained from the program (red) plotted along with the results obtained from the mathematical calculations in *Authier* [6] (blue). The plots display the reflectivities calculated while varying

ω , the rotation angle of the crystal. It is clear the two calculations are highly correlated, inferring the usefulness and accuracy of this multi-beam simulation program.

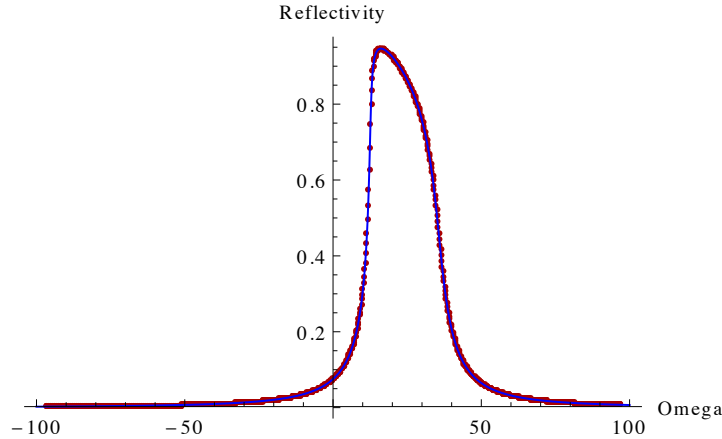


Figure 9: Gallium Arsenate (*GaAs*)

Germanium and Silicon are both crystalline materials such that the structure factor values from the reflection (a, b, c) are equal to that of the negative reflection $(-a, -b, -c)$. This provided no information as to the structure of the structure factor matrices essential in the multi programs calculations of reflectivity. Thus a new test was necessary with a different material - Gallium Arsenate, which has structure factors of (a, b, c) and $(-a, -b, -c)$ that differ, allowing a comparison with the program *Crystallography* to determine the structure of the amplitude and phases matrices.

Clearly the simulations made with the program *Multi* and the program *Crystallography* give analogous results for all of the elements tested, implying the program *Multi* can be utilised effectively in simulating n-beam X-ray diffraction.

3.2.1. Future Work

One problem with running the program in *xterm* is that it may be different platform used to when the program was originally being written. One example of this is having to make the change "MATLABEXPORT PAGER=LESS" in *xterm* before using the program. This change allows the program to properly load the parameter file for the user to view in the program. However, it would be more useful for this change to be implemented in the source code in the future.

Additionally, further investigation into the source code would be useful to solve the problem of certain files being unable to load, which could be due to a simple path error the program is trying to take. This would hopefully solve the problem of the program being unable to currently calculate structure factors individually. Although this was also due to the problem of missing *cromer* which was required to calculate both f and f' for the structure factor calculation, which could perhaps be implemented in an alternative way.

3.3. Creating a new Input file

To run the original *Multi* program, it is required to set all the variables required, for example the element, energy and reflections. These can all be set within the program, however this method can be slow, and the program will revert back to the previous settings without saving the users preferences upon reopening of the program if the user doesn't set the variables correctly. The input for the variables comes from two main files, *multi.inp* (input file) and *multi.ub* (UB matrix file), which the program reads and loads as variables, so it was thought to create a more efficient way to set these variables by writing a small function in *Mathematica* to produce both files from a single location. However, the first few lines of the file were space sensitive, with the program unable to load them and crashing when the number of characters or spaces were changed. Therefore the same filenames are used and same number of spaces inserted. A short function was written which, upon being presented with the required parameters all in one place in a single notebook, produced the two files *multi.inp* and *multi.ub* in the correct format such that *Multi* could read them. This worked well, however an improvement could be made to turn this function into a package. The function is listed in Appendix A. A next step would be presenting this function in the form of a Mathematica Package, making it more accessible and provide ease of implementation in the future.

References

- [1] S. Sample (2007), *X-Rays*. <http://science.hq.nasa.gov/kids/imagers/ems/xrays.html>. Retrieved September 2015.
- [2] P. Willmott (2011), *An Introduction to Synchrotron Radiation. Techniques and Applications*, John Wiley & Sons Ltd, UK. W. A. Hendrickson (2000), *Synchrotron crystallography*. Trends in Biochemical Sciences, 25 **12**, p637-643. <http://www.cell.com/cms/attachment/543998/3812514/gr1.jpg>
- [3] P. Barnes, S. Jaques and M. Vickers (1997), *Kinematic versus Dynamic Diffraction*. <http://pd.chem.ucl.ac.uk/pdnn/diff2/kinemat1.htm>. Retrieved September 2015.
- [4] A. Kamal (2015), *Miller Indecies*, <http://www.slideshare.net/AbeerKamal1/miller-indecies>. Retrieved September 2015.
- [5] M. Martinez=Ripoll (2015), *Crystallography*. http://www.xtal.iqfr.csic.es/Cristalografia/parte_06-en.html. Retrieved September 2015.
- [6] A. Authier (2001), *Dynamical Theory of X-Ray Diffraction*, Oxford University Press, United States.
- [7] B. W. Batterman and H. Cole (1964), *Dynamical Diffraction of X Rays by Perfect Crystals*, Reviews of Modern Physics, 36 **3**, p681-717.
- [8] R. Colella (1974), *Multiple Diffraction of X-rays and the Phase Problem. Computational Procedures and Comparison with Experiment*, Acta Crystallographica Section A, 30, p413-423.
- [9] J. Als-Nielsen and D. McMorrow (2001), *Elements of Modern X-Ray Physics*, John Wiley & Sons Ltd, UK.

Appendices

A. Mathematica Function

Listing 1: Multi Input File Generator (for notebook).

```
1  (* Multi_Input function to create two output files
2  multi.inp and multi.ub for the use of the programme
3  multi in calculating reflectivities *)
4
5  (*-----*)
6
7  SetDirectory[ "/home/barryrox/cryst/test"];
8  <<Crystallography`
9
10 (*-----*)
11 (* Function to write multi.inp and multi.ub Input
12 files. Set to a psi value of 1000. Set to Pi
13 Polarization (PiPol). *)
14 (* Input Variables (in order):
15 Nbeam - number of beams,
16 element - chosen element,
17 energy - in,
18 surfnorm - surface normal INTO the crystal {a,b,c},
19 refl1 - first reflection {a,b,c},
20 refl2 - second reflection {a,b,c},
21 crysthick - thickness of crystal in mm,
22 seminf - "T" for semi-infinite crystal, "F" if not,
23 omesteps - number of steps in the omega scan,
24 ome - lower limit (and actual value) of omega scan
25 value,
26 omescan - upper limit of omega scan value *)
27
28 GenerateMultiInput[Nbeam_,element_,energy_,surfnorm_,
29 refl1_,refl2_,crysthick_,seminf_,omesteps_,ome_,
30 omescan_] := Block[{SigPol,PiPol,LinPol,angle,EllPol,
31 compamp,refvect,deg,wvlngth,wvlngthscan,reciplattice,
32 crystthick,SF0,SF0R,SF0I,SF1,SF1neg,SF2,SF2neg,SFA01,
33 SFA02,SFA10,SFA20,SFA12,SFA21,SFP01,SFP02,SFP10,
34 SFP20,SFP12,SFP21,SFAmp,SFPhas},
35 SigPol="F";
36 PiPol="T";
37 LinPol="F";
38 angle=90;
39 EllPol="F";
40 compamp="1";
41 reflvect={0,0,0};
```

```

42 deg=Pi/180;
43 wvlngth=NumberForm[Lambda[energy],5];
44 wvlngthscan=NumberForm[Lambda[energy]+0.1,5];
45 reciplattice=NumberForm[1/(element[[2,2,1,1]]),
46 {11,10}];
47 SF0=CalcFH[element,energy,refvect];
48 SF0R=NumberForm[Re[SF0],{6,3}];
49 SF0I=NumberForm[Im[SF0],{6,3}];
50 SF1=CalcFH[element,energy,refl1];
51 SF1neg=CalcFH[element,energy,-refl1];
52 SF2=CalcFH[element,energy,refl2];
53 SF2neg=CalcFH[element,energy,-refl2];
54 SFA01=NumberForm[Abs[SF1],{6,3}];
55 SFA02=NumberForm[Abs[SF2],{6,3}];
56 SFA10=NumberForm[Abs[SF1neg],{6,3}];
57 SFA20=NumberForm[Abs[SF2neg],{6,3}];
58 SFA12=NumberForm[Abs[CalcFH[element,energy,
59 refl2-refl1]],{6,3}];
60 SFA21=NumberForm[Abs[CalcFH[element,energy,
61 refl1-refl2]],{6,3}];
62 SFP01=NumberForm[Mod[Arg[SF1]/deg,360],{6,3}];
63 SFP02=NumberForm[Arg[SF2]/deg+360,{6,3}];
64 SFP10=NumberForm[Arg[SF1neg]/deg+360,{6,3}];
65 SFP20=NumberForm[Arg[SF2neg]/deg+360,{6,3}];
66 SFP12=NumberForm[Arg[CalcFH[element,energy,
67 refl2-refl1]]/deg,{6,3}];
68 SFP21=NumberForm[Arg[CalcFH[element,energy,
69 refl1-refl2]]/deg,{6,3}];
70 SFAmp={{0,SFA01,SFA02},{SFA10,0,SFA12},{SFA20,
71 SFA21,0}};
72 SFPhas={{0,SFP01,SFP02},{SFP10,0,SFP12},{SFP20,
73 SFP21,0}};
74 And[Export["multi.ub",
75 Join[Inverse[CoordinateSystem/.element],
76 {""},
77 {"Transponierte UB      !!!!!"}],
78 "Table"],
79 Export["multi.inp",
80 Join[{"multi.inp
81                                     : this filename"},
82 {"multi.prt
83                                     : genaral data
84 file"},
85 {"multi.refl
86                                     : file for
87 reflectivities"}],

```



```

88 {"multi.trans
89                                     : file for
90 transmittivities"},
91 {"multi.3D1
92                                     : 1. file for mesh
93 scans"},
94 {"multi.3D2
95                                     : 2. file for mesh
96 scans"},
97 {"multi.ub
98                                     : file name of
99 orientation matrix"},
100 {"02
101                                     : OM=02, 01=03,
102 to select lorentz point"},
103 {{Nbeam ,"      : n-beam case      "}},
104 {{crysthick,"      : crystal thickness in mm"}},
105 {{seminf,"      : T = semi infinite crystal"}},
106 {{ SFOR,SFOI,"      : F(0) real and imaginary part"},
107 { , , }},
108 {{surfnorm[[1]],surfnorm[[2]],surfnorm[[3]] ,
109 "      : surface normal (into the crystal)},{ , , }},
110 {{omesteps,ome,omescan,"      : omega scan parameter"}},
111 {{1000,-1000,1000,"      : psi scan parameter"}},
112 {{0,wvlgth,wvlgthscan,"      : energy scan parameter"},
113 { , , }},
114 {"  h k l  list of all reflections      (n-beam - 1)
115 -----"},
116 {refl1,refl2,{ , , }},
117 {" ----- matrix of structure factor amplitudes
118 -----"},
119 Transpose[SFAmp],
120 {{ }},{ " ----- matrix of structure factor phases
121 -----"}},
122 Transpose[SFPhas],
123 {{ }},{ " ----- Polarization parameters -----"}},
124 {{ "Sig.Pol","Pi.Pol","Lin.Pol","Ell-Pol"},
125 {SigPol,PiPol,LinPol,EllPol},{ , ,angle,compamp}},
126 {{ }},{ " --- List of output Parameters -----"}},
127 {{ "mesh-3D1","mesh-3D2","transmittivities"},
128 {"T","T","F"},{2,3,}}
129 ],
130 "Table"]]]];

```